J. Biochem. **139**, 645–654 (2006)
doi:10.1093/jb/mvj074

Preparation and Characterization of a Novel Rice Plant–Specific Kinesin

Nobuhisa Umeki[1], Toshiaki Mitsui[1,*], Nozomi Umezu[2], Kazunori Kondo[2] and Shinsaku Maruta[2,*]

[1]Laboratories of Plant and Microbial Genome Control, Graduate School of Science and Technology, Niigata University, Niigata 950-2181; and [2]Division of Bioengineering, Graduate School of Engineering, Soka University, Hachioji, Tokyo 192-8577

Received October 19, 2005; accepted January 29, 2006

Kinesin is an ATP-driven motor protein that plays important physiological roles in intracellular transport, mitosis and meiosis, control of microtubule dynamics, and signal transduction. The kinesin family is classified into subfamilies. Kinesin species derived from vertebrates have been well characterized. In contrast, plant kinesins have yet to be adequately characterized. In this study, we expressed the motor domain of a novel rice plant-specific kinesin, K16, in *Escherichia coli*, and then determined its enzymatic characteristics and compared them with those of kinesin 1. Our findings demonstrated that the rice kinesin motor domain has different enzymatic properties from those of well known kinesin 1.

Key words: fluorescence, kinesin, kinetics, motility, plant.

Abbreviations: DTT, dithiothreitol; EDTA, ethylendiaminetetraacetic acid; EGTA, ethylene glycol bis(β-aminoethyl ether)-*N,N,N′,N′*-tetraacetic acide; HEPES, 2-[4-(2-hydroxyethyl)-1-piperazinyl]ethane sulfonic acid; IPTG, isopropyl-β-D-thiogalactopyranoside; K16, rice-specific kinesin; K16MD, rice-specific kinesin motor domain; KIFs, kinesin superfamilies; MKH350, mouse kinesin head domain; MOPS, 3-(*N*-morpholino)propanesulfonic acid; MT, microtubule; NBD-ATP, 2′(3′)-*O*-[6-(*N*-(7-nitrobenz-2-oxa-1,3-diazol-4-yl)amino)hexanoic]-ATP; Ni-NTA, nickel nitrilo triacetic acide; ORF, open reading frame; PCR, polymerase chain reaction; P_i, phosphate; PIPES, 1,4-piperazinediethanesulfonic acid; PMSF, phenylmethylsulfonyl fluoride; SDS-PAGE, sodium dodecyl sulfate polyacrylamide gel electrophoresis.

Kinesins constitute a superfamily of ATP-driven microtubule motor proteins (KIFs) found in all eukaryotic organisms. Kinesins perform many diverse cellular functions such as in the transport of organelles and vesicles, spindle formation and elongation, chromosome segregation during cell division, microtubule dynamics, and morphogenesis (*1–5*). A common characteristic of KIFs of eukaryotic phyla is a highly conserved motor domain (30–40% identity) of approximately 350 residues, which contains an ATP-binding site and a microtubule-binding site. Outside the motor domain, KIFs show less sequence homology (*1*, *4*, *6–9*). However, it has been shown that interactions occur in a region outside the motor domain. Moreover, Hirokawa *et al.* demonstrated that several KIFs become attached to specific cargoes through interactions with adaptor proteins in these regions (*9–13*). Therefore, it is thought that these regions are related to individual distinguishing functions of each kinesin.

Kinesin superfamilies in animals have been well studied, especially those in mouse and human (*9*, *11*, *13–16*). The identification of all KIFs was confirmed by a database search of the total human genome, 45 KIFs being found (*16*). In contrast, only a few kinesins have been characterized in plants, including in *Arabidopsis thaliana* (*17–21*). The complete sequencing of the *Arabidopsis* genome led to the identification of 61 kinesin-like genes which is the largest number of kinesins that have been sequenced among all eukaryotic genomes (*22*). Phylogenetic analysis of *Arabidopsis* kinesin motor domain sequences with other motor domain sequences revealed that some of them do not belong to any known family, and that some subfamilies are unique to *Arabidopsis* and maybe to plants. These plant-specific kinesins may participate in specific plant functions, including the formation of phragmoplasts evident at cell division, morphogenesis of the leaf trichome, flower morphogenesis, and rapid movement of Golgi stacks seen in plants. Kinesins found in the tobacco pollen tube have also been characterized at the biochemical (*23*) and molecular (*24*) levels.

Recently, the genome sequences of both the rice *japonica* and *indica* sub-species have been completed using the random-fragment shot gun sequence method (*25*, *26*). It is of interest to determine whether rice kinesins also belong to subfamilies unique to rice and other plants. Our preliminary analysis of the rice genome sequence revealed that rice has a similar number of kinesins to *Arabidopsis*. We focused on kinesins specifically found in the rice genome. In the present study, we searched for plasmids encoding rice-specific kinesins in a cDNA library of rice, and obtained 6 rice kinesin cDNAs from the National Institute of Agrobiological Sciences (NIAS). One of these kinesins, kinesin K16, was expressed in *E. coli* and its enzymatic characteristics studied. Rice kinesins apparently showed different characteristics, especially in the affinities for ADP and microtubules, from those of conventional kinesins, suggesting rice-specific properties. To our knowledge, this is the first report describing the characterization of a rice kinesin.

*To whom correspondence should be addressed. Fax: +81-426-91-9312, E-mail: shinsaku@t.soka.ac.jp (Shinsaku Maruta); Fax: +81-25-262-6641, E-mail: t.mitsui@agrews.agr.niigata-u.ac.jp (Toshiaki Mitsui)

MATERIALS AND METHODS

Chemicals—Restriction enzymes and other enzymes were purchased from Toyobo (Tokyo) unless otherwise stated. Oligonucleotides were synthesized by Sawady (Tokyo). The Ni-chelating column was from Sigma (St. Louis, MO). *Escherichia coli* BL21(DE3)pLysE and the pET21a vector were from Novagen (Madison, WI). Chemicals were purchased from Wako Pure Chemicals (Osaka) unless otherwise described. ATP and ADP were purchased from Oriental Yeast (Osaka). The BCA protein concentration assay reagent was from Pierce (Rockford, IL).

Molecular Biology—Polymerase chain reaction (PCR) was carried out with a PROGRAM TEMP CONTROL SYSTEM PC-700 (ASTEC), PROGRAM TEMP CONTROL SYSTEM PC-800 (ASTEC), or QUICK THERMO II (Nippon Genetics, Tokyo). Gel electrophoresis, transformation, and restriction enzyme digestion were performed as described in Molecular Cloning (Cold Spring Harbor Laboratory Press, 2001). The recovery of DNA fragments from agarose gels was carried out with a DNA Gel Extraction Kit (Millipore, Bedford, MA). DNA ligation was performed with a DNA Ligation Kit Ver.2 (Takara Shuzo, Ohtsu, Japan) according to the manufacture's instructions. *E. coli* DH5α was used for transformation for plasmid DNA preparation.

Cloning of the Rice Kinesin Motor Domain—The K16 plasmid (accession No. AK068672) was supplied from the National Institute of Agrobiological Sciences (NIAS). A DNA fragment encoding amino acids 77–419 of the predicted 343 residue K16MD was synthesized by PCR from the LambdaFLC-K16 plasmid using forward and reverse primers 5′-CAAAGCTAGCGACCCGGCGCCCAAGGAGAATGTCA-3′ and 5′-CAAACTCGAGCTTTATTAAAGATTTTTCATCTATAA-3′, respectively. The 5′-PCR oligonucleotide consisted of *Nhe*I and corresponded to eight amino acids (D77–V84) of the K16 protein. The 3′-PCR oligonucleotide consisted of 24 bases corresponding to amino acids I412–K419 of the K16 protein followed by a *Xho*I site. Four extra bases were added to each primer at the restriction site to enhance binding at *Nhe*I and *Xho*I restriction sites. The gel-purified PCR fragment was cloned into the pET21a expression vector using *Nhe*I and *Xho*I restriction sites. The cDNA sequence was confirmed by the dideoxy chain termination method with a SQ-5500 sequencer (Hitachi, Tokyo) using the Genetyx program (Software Development).

Kinesin Expression—E. coli BL21(DE3)pLysE was transformed with pET21a::K16MD for large scale expression of the recombinant kinesin protein. Transformants were selected on L-plates with 100 μg/ml ampicillin. For protein purification, *E. coli* was grown at 37°C and 200 rpm for 5 h in 6 liter L-broth containing 100 μg/ml ampicillin to an absorbance value at 600 nm of 1.2, 0.1 mM IPTG and 0.1 mM DTT were added, then incubation was continued at 37°C for 4 h. These cells were centrifuged at 4,700 × *g* for 20 min in a Rotor 30 (HITACHI Himac CR22G) and then suspended in HEM buffer (10 mM HEPES, pH 7.2, 1 mM $MgCl_2$, 1 mM EGTA, 25 mM NaCl, and 1 mM DTT) prior to storage at –80°C until use. The frozen cells were thawed and suspended in 20 ml lysis buffer for a Ni-column (100 mM Tris-HCl, pH 7.8, 300 mM NaCl, 0.1 mM leupeptin, 0.1 mM PMSF, and 0.1 mM DTT) and then sonicated for 5 min (5 times, sonication for 30 s and on ice for 30 s) at Micro tip limit 5 and Duty cycle 40% with an ULTRAS HOMOGENIZER VP-30S (TAITEC). The sample was clarified by centrifugation at 200,000 × *g* for 1 h in a 70Ti (BECKMAN L8-70M Ultra-centrifuge, Beckman, Fullerton, CA). The supernatant was stored at 4°C until use.

Purification of Recombinant Rice Kinesin Motor Domain (K16MD)—The stored supernatant was loaded on a Ni-NTA column, which had been equilibrated with native buffer (300 mM NaCl, 100 mM Tris-HCl, pH 7.5, and 0.2 mM β-mercaptoethanol). The column was washed with native buffer, and then with native buffer containing 50 mM imidazole-HCl, pH 7.5. The desired protein was eluted with 100 mM Imidazole-HCl, pH 7.5, in native buffer, and the fractions containing kinesin were pooled. Purity was assessed by sodium dodecyl sulfate polyacrylamide gel electrophoresis (SDS-PAGE), which gave a single band on Coomassie-stained gels. Samples were dialyzed against 120 mM NaCl, 30 mM Tris-HCl, pH7.5, and 1 mM DTT, and stored at –80°C until use.

Preparation of MKH350—The expression plasmid for the pET15b::MKH350 was constructed by PCR, and its sequence was confirmed by the dideoxy chain termination method with a SQ-5500 sequencer (Hitachi, Tokyo) using the Genetyx program (Software Development) (*14*). The expression plasmid was transformed into *E. coli* BL21(DE3). Bacterially expressed protein was purified as described above.

SDS-PAGE—Protein analysis was performed in 7.5–20% polyacrylamide gradient slab gels in the presence of 0.1% SDS at a constant voltage (200 V) in the discontinuous buffer system of Laemmli (*27*). Peptide bands were visualized by staining with Coomassie Brilliant Blue. The molecular masses of the peptide bands were determined by comparing their mobilities with those of markers of known molecular weight.

Purification and Polymerization of Tubulin—Tubulin was purified from porcine brain as described by Hackney (*28*). To polymerize the tubulin (in 100 mM Pipes, pH 6.8, 1 mM EGTA, 1 mM $MgCl_2$, and 1 mM GTP), it was incubated for 30 min at 37°C, and then taxol was added to a final concentration of 10 μM. The taxol-stabilized microtubules (MTs) were pelleted by centrifugation at 200,000 × *g* for 15 min at 37°C (HITACHI Himac CS120GX), the supernatant was aspirated off, and the MT pellet was carefully washed with buffer (100 mM Pipes, pH 6.8, 1 mM EGTA, 1 mM $MgCl_2$, 1 mM GTP, and 10 μM taxol). For MT pelleting assays, the MTs were suspended in buffer (20 mM MOPS, pH 7.0, 1 mM DTT, 5 mM $MgCl_2$, 25 mM NaCl, and 20 μM taxol). All MT concentrations described below are the concentrations of tubulin heterodimers.

ATPase Assay—1 μM K16MD and 1 μM MKH350 were pre-incubated for 5 min in 10 mM imidazole-HCl, pH 7.0, 50 mM KCl, 3 mM $MgCl_2$, 0.1 mM EDTA, 1 mM EGTA, 1 mM β-mercaptoethanol and 5 μM microtubules. The ATPase reaction was initiated by the addition of 2 mM ATP at 25°C and terminated by the addition of 10% trichloroacetic acid. The released P_i was measured by the method of Youngburg and Youngburg (*29*).

MT Pelleting Assays—Pelleting assays were performed according to the method described by Lockhart *et al.* (*30*). Briefly, 7 μM K16MD in buffer (20 mM MOPS, pH 7.2, 1 mM DTT, 5 mM $MgCl_2$, 25 mM NaCl, and 20 μM

taxol) was mixed with 5 mM ATP and 5 mM ADP, and then the mixture was allowed to stand for 10 min at 25°C. Subsequently, 0–35 μM MTs was added, and the solution was gently mixed prior to incubation (10 min, 25°C) and centrifugation (200,000 × *g*, 20 min, 25°C) (Himac RP100AT3, Hitachi). The supernatants and pellet were applied to SDS slab gels and stained with Coomassie Brilliant Blue.

Fluorescence Measurement of Rice Kinesin-NBD-ATP—Fluorescence was measured at 25°C with a spectrofluorometer F-2500 (HITACHI, Tokyo). The fluorescent ATP analogue, NBD-ATP was synthesized according to Maruta *et al.* (*31*). Changes in the fluorescence intensity of 0.3 μM NBD-ATP in the presence of 1.5 μM K16MD on the addition of nucleotides were monitored in a solution comprising 30 mM Tris-HCl, pH 7.5, 120 mM NaCl, and 2 mM $MgCl_2$. The excitation and emission wavelengths for NBD-ADP were 475 nm and 535 nm, respectively.

Fluorescence Stopped-Flow Measurements—Fluorescence stopped-flow measurements were carried out with an SX-18MV (Applied Photo Physics) stopped flow apparatus with an excitation wavelength of 475 nm at 20°C. For the emission, a cut-off filter of 525 nm was used. The nucleotide to protein ratio was kept at 5. The buffer conditions were as follows: 40 mM NaCl, 20 mM Tris-HCl, pH 7.5, and 1 mM $MgCl_2$.

RESULTS

Nucleotide and Deduced Amino Acid Sequences of K16—The nucleotide and deduced amino acid sequences of K16 are shown in Fig. 1. The full-length cDNA comprised 3,316 bp with an open reading frame (ORF) starting at nucleotide position 92 and ending with a stop codon at nucleotide 1735. The predicted protein comprised 547 amino acid residues with an estimated molecular weight of approximately 60 kDa. A search of sequence databases with the predicted amino acid sequence using BLAST searches revealed that a region of approximately 340 amino acids in full-length K16 is a motor domain. The motor domain of K16 (K16MD) comprises 343 amino acid residues with an estimated molecular weight of approximately 38 kDa and contains several regions that exhibit almost complete conservation of amino acid sequences among all known kinesin family members, *i.e.*, L1 (RXRP), which interacts with the base, the phosphate-binding loop (GXXGXGKT/S), the switch I region (NXXSSRSH), the switch II region (DLAGXE), and the microtubule-binding site (*32*). The amino acid sequence of K16MD showed approximately 43.2% similarity with that of the motor domain of mouse kinesin. However, the region other than the motor domain exhibited no similarity with other kinesin-family members.

Preparation of K16 Motor Domain—To study the properties of the K16 motor domain, a polypeptide corresponding to amino acids D77–K419 was expressed in *E. coli* and purified. A DNA fragment encoding the 343 amino acids of K16MD was generated by PCR as described. A DNA fragment was ligated to the vector pET21a, which had been digested with *Nhe*I and *Xho*I. The resulting chimeric plasmid generates a fusion protein in which the kinesin insert is fused at the C-terminus to a sequence of six histidine residues, which permits affinity purification on Ni-NTA agarose. As shown in Fig. 2, K16MD was eluted as peak C from the Ni-NTA agarose column on the addition of 100 mM imidazole. Its separation from the other proteins of *E. coli* was analyzed by SDS-PAGE, which showed that the peak C fractions only contained highly pure kinesin (Fig. 2). Approximately 30 mg of pure K16MD could be prepared from 6 liters of culture by the procedure described above. As shown in Fig. 2B, SDS-PAGE gave a single band corresponding to approximately 38 KDa, which was consistent with the molecular mass of K16MD calculated from the deduced amino acid sequence.

ATPase Activity—The basal ATPase activity and microtubule-activated ATPase activity of K16MD and the mouse kinesin head domain (MKH350) were measured. As shown Table 1, in the absence of MTs, the basal steady-state ATPase activity of K16MD was slightly lower (1.62 P_i mol/site mol/min) than that of MKH350 (2.52 P_i mol/site mol/min) and that of bovine brain kinesin (2.40 P_i mol/site mol/min). In the presence of MTs, the ATPase activity of K16MD was enhanced by approximately ten-fold. However, the magnitude of the enhancement of K16MD ATPase activity by MTs was much lower than that for mouse brain kinesin. These results suggest that the interaction of K16MD and microtubules is weaker than that of mouse brain kinesin.

Therefore, the MT concentration dependency of the ATPase activity of K16MD was examined. The ATPase activity was activated by microtubules in a concentration-dependent manner (Fig. 3). The maximum activity was approximately 51.5 mol/site mol/min (*i.e.*, more than 30-fold activation) and the half-maximum ATPase activation [K_m (MT)] was about 5 μM in the low ionic strength buffer [30 mM Tris-HCl, pH 7.5, 3 mM $MgCl_2$, 0.1 mM EDTA, 1 mM EGTA, 1 mM β-mercaptoethanol, and 1 μM K16MD]. Thus, K16MD has a lower V_{max} and higher K_m (MT) than mouse kinesin.

The ionic and pH dependence of the ATPase activity of K16MD were investigated in the presence and absence of microtubules. The degree of activation was sensitive to the ionic concentration, 0–150 mM NaCl, as shown in Fig. 4. As to pH dependency, K16MD exhibits maximum basal ATPase activity at pH 5.5 at 25°C, but the maximum microtubule-activated ATPase activity was observed at pH 6.0 (Fig. 5).

MT Pelleting Assays—To investigate the interaction of K16MD and MTs, microtubule pelleting assays were performed. In equilibrium binding experiments, 7 μM K16MD was incubated with various concentrations of microtubules (0–35 μM) in the presence or absence of nucleotides. The results were compared with those for MKH350. The levels of K16MD and MKH350 bound to microtubules were estimated from the SDS-PAGE protein bands. As shown in Fig. 6, in the absence of nucleotides, approximately 75% of MKH350 found in the pellet contained 15 μM microtubules. In the presence of nucleotides, approximately 65% and 55% of MKH350 for ATP and ADP, respectively, was found in the pellet. In contrast, about 60% of K16MD was found in the pellet in the absence of nucleotides. In the presence of nucleotides, approximately 45% and 25% of K16MD for ATP and ADP, respectively, was found in the pellet. From the data in Figure 6, the maximum occupancy and the dissociation constants (K_{MT}) in the presence and absence of nucleotides for the kinesins were also estimated. The maximum occupancy (%)

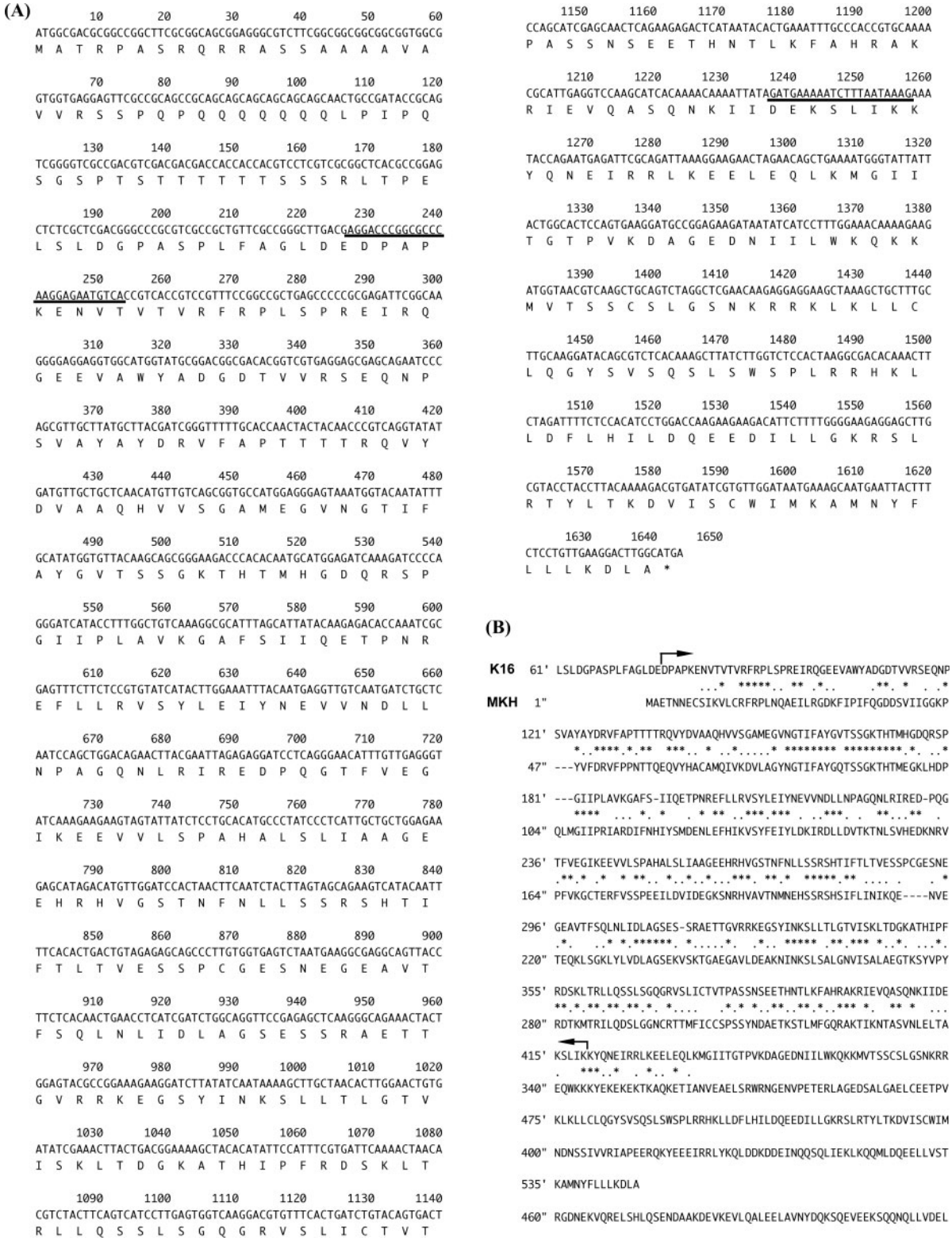

Fig. 1. **Nucleotide and deduced amino acid sequences of rice kinesin K16.** (A) Nucleotide and deduced amino acid sequences of rice kinesin K16. The nucleotide sequence is shown on the upper line and the deduced amino acid sequence on the lower line. The pair of primers is underlined. (B) Sequence homology of rice kinesin with mouse kinesin (MKH350). Identical amino acids are indicated by asterisks and similar amino acids by dots. Gaps are indicated by dashed lines. A pair of arrows shows the motor domain region of rice kinesin. The deduced rice kinesin amino acid sequence is shown on the upper line and the deduced MKH350 amino acid sequence on the lower line. A sequence homology search revealed that the rice kinesin motor domain (77–419 aa) xhibits 43.2% homology to that of MKH350 at the amino acid level. A homology search was performed using the GENETYX-MAC software (Software Development, Tokyo).

Table 1. **ATPase activity of K16MD and MKH350.** 1 μM K16MD and 1 μM MKH350 were preincubated for 5 min in 10 mM imidazole-HCl, pH 7.0, 50 mM KCl, 3 mM $MgCl_2$, 0.1 mM EDTA, 1 mM EGTA, 1 mM β-mercaptoethanol, and 5 μM microtubules. The ATPase reactions were started by adding 2 mM ATP at 25°C.

	Hydrolysis (P_i-mol/kinesin-mol/min)	
	–MTs	+MTs
K16MD	1.62	16.2
MKH350	2.52	114.5

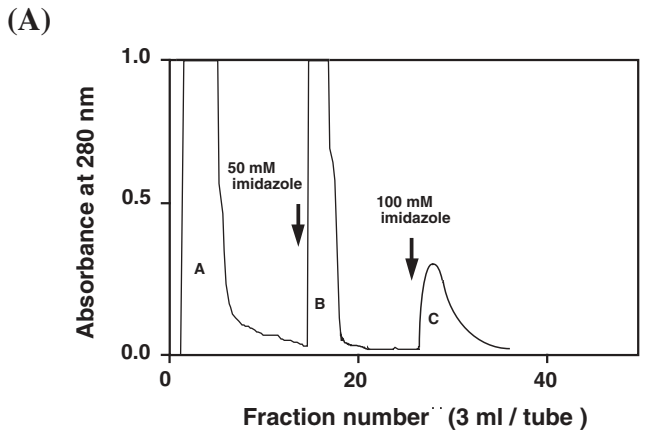

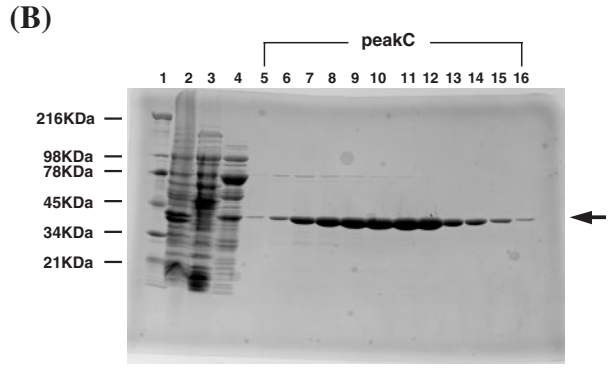

Fig. 2. **Affinity purification of rice kinesin protein on Ni-NTA agarose.** (A) After loading of the sample, the column was washed for 1 h at 2 ml/min with native buffer (120 mM NaCl, 30 mM Tris-HCl, pH 7.5, and 0.2 mM β-mercaptoethanol) and subsequently with 50 mM imidazole-HCl, pH 7.5, in native buffer. The desired protein was eluted with 100 mM imidazole-HCl, pH 7.5, in native buffer. Fractions (3 ml) were collected and the ultraviolet-absorbing fractions of peak C were pooled. (B) Purity was assessed by SDS gel electrophoresis, which gave a single band on Coomassie-stained gels. Lane 1, molecular weight markers; lane 2, precipitate of lysate; lane 3, one fraction of peak A in A; lane 4, one fraction of peak B; lanes 5–16, whole fractions of peak C. The arrow indicates the rice kinesin motor domain, 38 kDa.

and K_{MT} for K16MD in the absence of nucleotides, and in the presence of ATP and ADP were (99%) 14.3 μM, (70%) 22.5 μM, and (60%) 25 μM, respectively. On the other hand, The values for MKH350 were (100%) 8.7 μM, (95%) 10.9 μM, and (90%) 19.6 μM, respectively. These results clearly indicate that the interaction of K16MD and microtubules is weaker than for MKH350, which is consistent with the results for microtubule-enhanced ATPase activity.

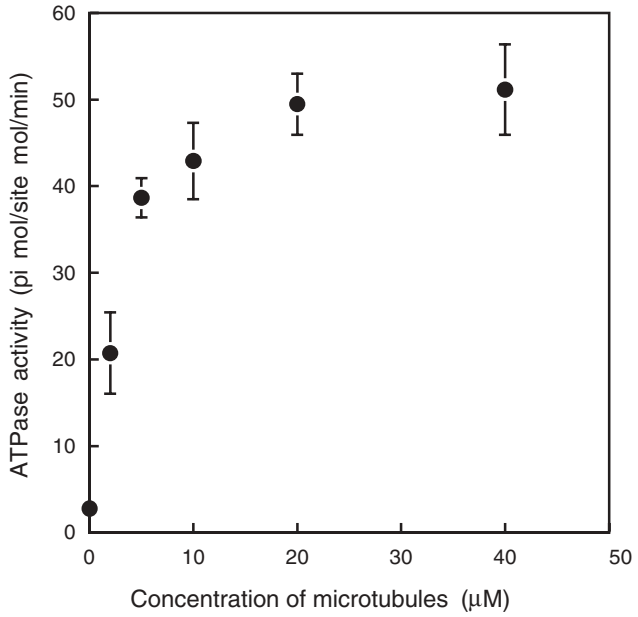

Fig. 3. **Microtubule concentration dependence of the ATPase activity of K16MD.** ATPase assays were carried out at 25°C in 30 mM Tris-HCl, pH 7.5, 3 mM $MgCl_2$, 0.1 mM EDTA, 1 mM EGTA, 1 mM β-mercaptoethanol, 1 μM K16MD, and 0–40 μM microtubules. The ATPase reaction was started by adding 2 mM ATP.

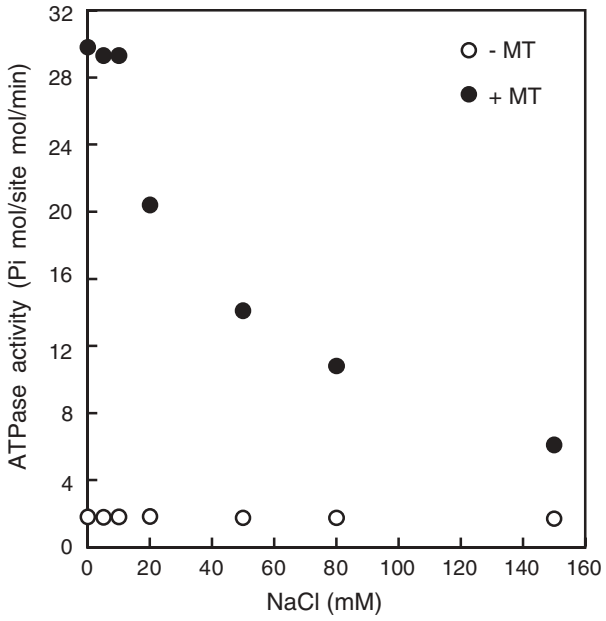

Fig. 4. **NaCl concentration dependence of the ATPase activity of K16MD.** ATPase assays were carried out at 25°C in 30 mM Tris-HCl, pH 7.5, 0–150 mM NaCl, 3 mM $MgCl_2$, 0.1 mM EDTA, 1 mM EGTA, 1 mM β-mercaptoethanol, and 1 μM K16MD, in the absence (open circles) or presence (closed circles) of 5 μM microtubules. The ATPase reaction was started by adding 2 mM ATP.

Interaction of K16MD with NBD-ADP-K16MD— We employed a fluorescent ATP analogue, 2′(3′)-*O*-{6-(*N*-(7-nitrobenz-2-oxa-1,3-diazol-4-yl)amino)hexanoic}-ATP (NBD-ATP), to monitor the formation of the transient

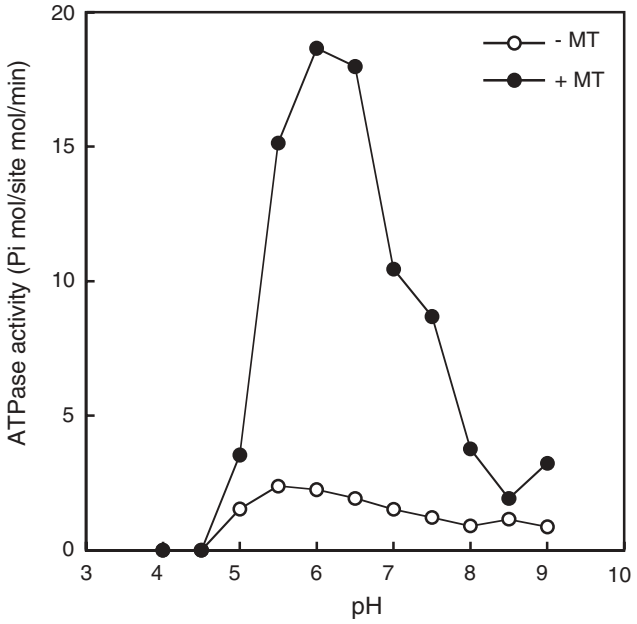

Fig. 5. **pH dependence of the ATPase activity of K16MD.** ATPase assays were carried out at 25°C in 50 mM NaCl, 3 mM $MgCl_2$, 0.1 mM EDTA, 1 mM EGTA, 1 mM β-mercaptoethanol, and 1 μM K16MD, in the absence (open circles) or presence (closed circles) of 5 μM microtubules. The ATPase reaction was started by adding 2 mM ATP. For pH 4.0–5.0, acetate-NaOH; for pH 5.5–6.5, MES-NaOH; for pH 7.0–7.5, MOPS-NaOH; and for pH 8.0–9.0, Tris-HCl were used as buffers.

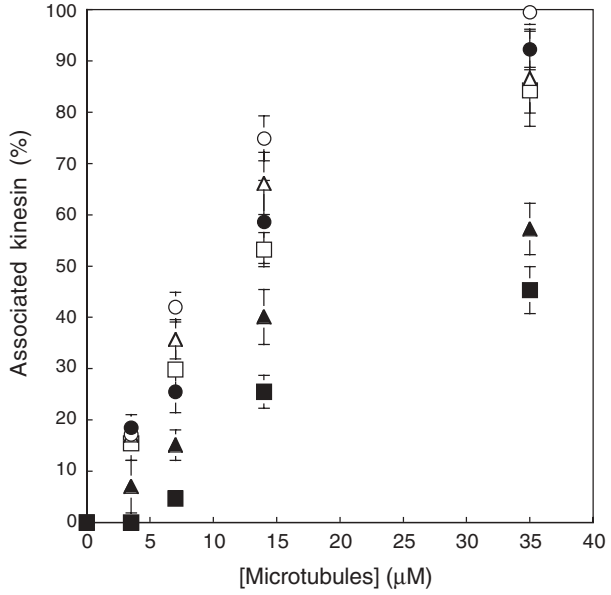

Fig. 6. **Microtubule pelleting assay.** The buffer conditions were as follows; 20 mM MOPS, pH7.2, 1 mM DTT, 5 mM $MgCl_2$, 25 mM NaCl, and 20 μM taxol at 25°C. To 7 μM rice-kinesin, 5 mM ATP, 5 mM ADP, no nucleotide and 0–35 μM MT were added. After centrifugation, the supernatant and pellet were subjected to SDS-PAGE. The ratio of associated rice kinesin to MT was estimated by densitometric analysis of the protein-stained SDS-PAGE gel. Association constant (%) = 100 − (the concentration of rice kinesin in the supernatant in the absence or presence of nucleotides)/(the concentration of rice kinesin in the supernatant in the absence of nucleotides and MT) × 100. Band intensities were determined with an image analyzer. Closed circles, K16MD; closed triangles, K16MD + ATP; closed squares, K16MD + ADP; open circles, MKH350; open triangles, MKH350 + ATP; open squares, MKH350 + ADP.

intermediate of K16MD ATPase. NBD-ATP carries a NBD fluorophore at 2′ or 3′ of ribose *via* an aminohexanoic spacer, which is highly sensitive to environmental conditions. Upon the addition of 1.5 μM K16MD to 0.3 μM NBD-ATP (under single-turnover conditions), the fluorescence intensity at 535 nm resulted in an immediate increase of approximately three-fold in NBD fluorescence (Fig. 7). Subsequently, the fluorescence intensity did not significantly change due to the hydrolysis of NBD-ATP to NBD-ADP. The fluorescence intensity completely recovered to the initial level on the addition of 1 mM ATP. These results suggest that enhancement of NBD-ATP fluorescence reflects the binding of NBD-ATP to the ATP binding site of K16MD.

Stopped-Flow Experiments on NBD-ATP Binding to K16MD—The first phase of binding of NBD-ATP to K16MD under pseudo first order conditions with [NBD-ATP] > [K16MD] was examined by stopped-flow measurement. The nucleotide to protein ratio was kept at 5 as a compromise between achieving strictly first-order kinetics and maintaining a measurable fluorescence change relative to the background signal. NBD-ATP binding resulted in increasing NBD-ATP fluorescence intensity (Fig. 8). The time course of the increase in NBD-ATP fluorescence was identical for successive pushes in the stopped-flow apparatus. The data best fitted a double exponential curve. The biphasic behavior of NBD-ATP binding may be due to the presence of the 2′- and 3′-isomers of the ATP analogue in the solution (*31*). Similar biphasic behavior was reported previously for the interaction of kinesin 1 with a mixture of the 2′ and 3′-isomers of Mant-ATP

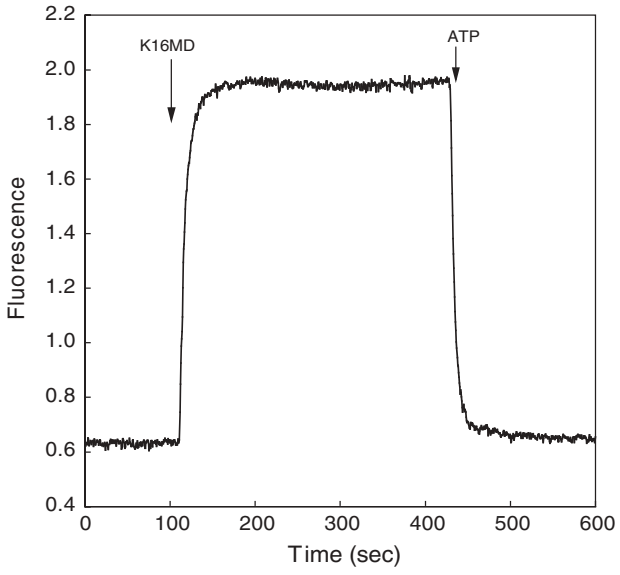

Fig. 7. **Serial changes in rice kinesin-NBD-ADP fluorescence on addition of ATP.** The changes in the fluorescence intensity of K16MD-NBD-ADP on the addition of nucleotides were monitored in a solution comprising 120 mM NaCl, 30 mM Tris-HCl, pH 7.5, 2 mM $MgCl_2$, and 1 mM DTT containing 0.3 μM NBD-ATP and 1.5 μM K16MD at 25°C. The excitation and emission wavelengths were 475 nm and 535 nm, respectively.

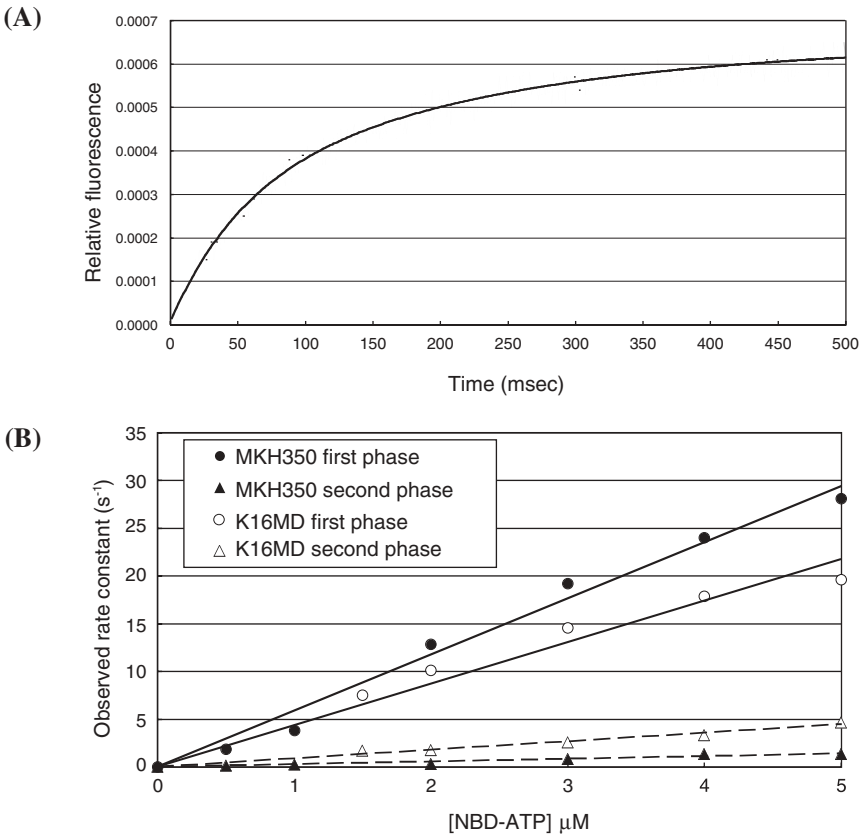

Fig. 8. **(A) Fluorescence transients observed upon addition of excess NBD-ATP (5 μM) to K16MD (1 μM) in the stopped-flow apparatus.** The buffer conditions were as follows: 40 mM NaCl, 20 mM Tris-HCl, pH7.5, and 1 mM $MgCl_2$ at 20°C. Zero time is the time at which the flow stopped. The superimposed lines are least mean squares fits to a double exponential curve. The reaction was monitored as to NBD fluorescence intensity. The fit of the data to a double exponential function provided the initial rapid phase (first phase) of fluorescence enhancement at 19.6 s^{-1} and the slower second phase at 4.65 s^{-1}. **(B) The exponential rate constants of the first and second phases increased linearly as a function of the NBD-ATP concentration from 0–5 μM NBD-ATP.** For K16MD, the data provided the second order rate constant for NBD-ATP binding, the initial fast phase at 4.35 μM^{-1} s^{-1} (open circles), and the second slow phase at 0.88 μM^{-1} s^{-1} (open triangles). For MKH350, the data provided the second order rate constant for NBD-ATP binding, the initial fast phase at 5.88 μM^{-1} s^{-1} (closed circles), and the second slow phase at 0.28 μM^{-1} s^{-1} (closed triangles).

(*33*). The second phase of NBD-ATP binding was slower than the first phase. For K16MD, with 5 μM NBD-ATP, the rate constants of the first and second phases were 19.60 and 4.65 s^{-1}, respectively. In contrast, for MKH350, with 5 μM NBD-ATP, the rate constants of the first and second phases were 28.13 and 1.34 s^{-1}, respectively. With low NBD-ATP concentrations (<5 μM), the observed rates of the first and second exponential phases increased linearly as a function of the NBD-ATP concentration. The data gave second order rate constants for the first phase for K16MD and MKH350 of 4.35 and 5.88 μM^{-1} s^{-1}, respectively. Moreover, the second order rate constants for the second phase for K16MD and MKH350 were 0.88 and 0.28 μM^{-1} s^{-1}, respectively. These data suggested that the affinity of NBD-ATP for K16MD is lower than that for MKH350.

Release of NBD-ADP from K16MD—Subsequently, we examined the kinetics of NBD-ADP release from K16MD. The dissociation of ADP from K16MD was monitored by measuring the fluorescence change of NBD-ATP. After complete hydrolysis of 0.3 μM NBD-ATP to NBD-ADP with 1.5 μM K16MD, the addition of 1 mM regular ATP resulted in a decrease in the fluorescence of NBD-ADP (Fig. 9), suggesting that NBD-ADP was released from the active site of K16MD through chasing with excess regular ATP. For K16MD, with 10 μM ATP, the rate constant was 0.035 s^{-1}. Figure 9B shows a plot of the rate constant of the dissociation of NBD-ADP from K16MD against the ATP concentration. The rate constant increased depending on the ATP concentration. In the absence of microtubules, the maximum rate constants of K16MD and MKH350 were 0.177 and 0.074 s^{-1}, respectively. Note that the maximum rate constant of K16MD was much higher than that of MKH350. This suggested that the affinity of NBD-ADP to K16MD is much lower than that of MKH350. Moreover, in the presence of microtubules, the maximum rate constants of K16MD and MKH350 were 0.214 and 0.155 s^{-1}, respectively. The maximum rate constant of MKH350 in the presence of microtubules was two-fold higher than that in the absence of microtubules. In contrast, for K16MD, the maximum rate constant in the presence of microtubules was slightly higher than that in the absence of microtubules.

DISCUSSION

The aim of the present study was to characterize a plant kinesin specifically found in the rice genome. Recently, draft sequences from both the *japonica* and *indica* sub-species were completed using the random-fragment shotgun sequence method (*25*, *26*). Furthermore, the international rice genome-sequencing project declared completion of the rice genome using a mapped clone sequencing strategy. Therefore, it was quite timely to search for kinesins in the rice genome. Kinesins are involved in diverse cellular functions. It is strongly expected that the kinesins found in the rice genome also have important cellular roles. In support of this notion, genomic studies of *Arabidopsis thaliana* revealed that *Arabidopsis* has at least 61 kinesin-like (kinesin-related) proteins and some of them do not fall into known subfamilies, and thus may be plant-specific (*22*). Interestingly, it has been revealed that *Arabidopsis*-specific kinesins are involved in the formation

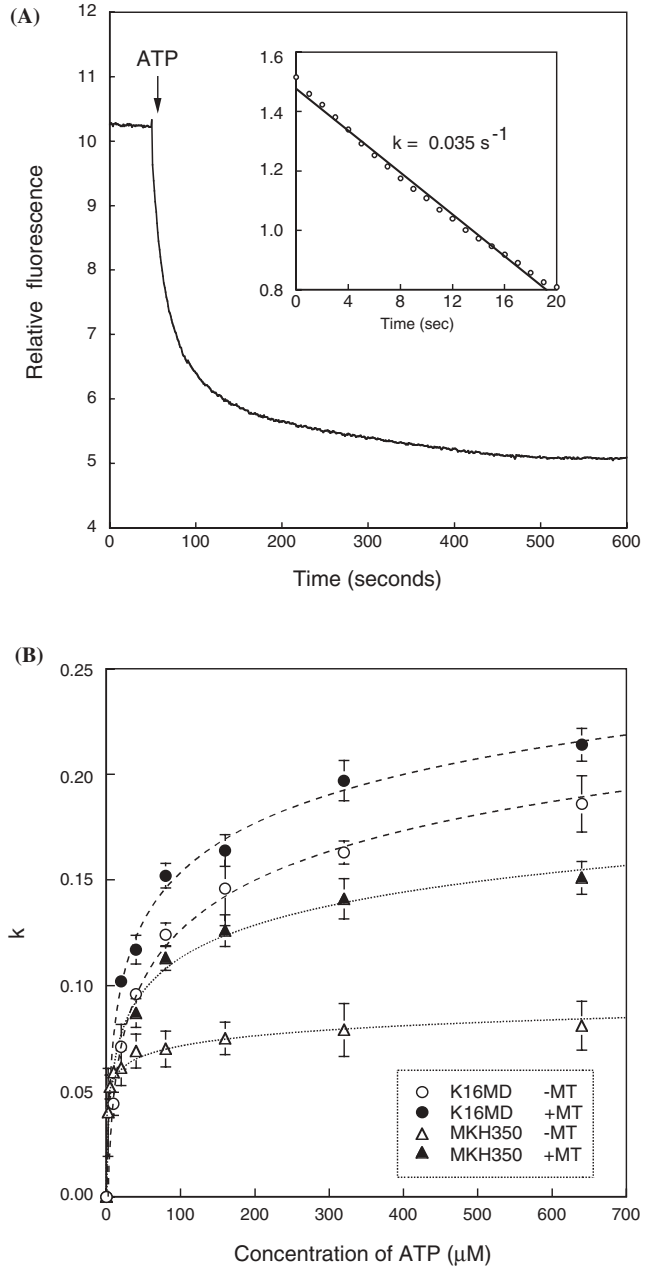

Fig. 9. **Release of NBD-ADP from the active site of K16MD.** (A) Fluorescence transients observed upon addition of excess ATP (10 μM) to the rice kinesin-NBD-ADP complex. The buffer conditions were as follows. 120 mM NaCl, 30 mM Tris-HCl, pH 7.5, 2 mM $MgCl_2$ at 25°C, in the absence of microtubules. 1.5 μM K16MD was premixed with 0.3 μM NBD-ATP and after complete hydrolysis of NBD-ATP to NBD-ADP. Changes in NBD-ADP fluorescence intensity were measured at 535 nm (excitation at 475 nm). The inset shows a semilog plot of the ATP-induced fluorescence change against time; $k = 0.035\ s^{-1}$. (B) Release of NBD-ADP from kinesins in the presence or absence of 1.5 μM microtubules. The ATP concentration–dependent rate constants of the release of NBD-ADP from K16MD and MKH350 were measured by monitoring fluorescence change of NBD-ADP. The values were determined under the same conditions as in (A). For K16MD, the maximum rate constants in the presence (closed circles) and absence (open circles) of microtubules were 0.214 s^{-1} and 0.177 s^{-1}, respectively. In contrast, for MKH350, the maximum rate constants in the presence (closed triangles) and absence (open triangles) of microtubules were 0.155 and 0.074 s^{-1}, respectively.

of the phragmoplasts seen on cell division (*34*, *35*), morphogenesis of the leaf trichome (*20*, *36*), and rapid movement of Golgi stacks (*20*).

We selected six cDNAs encoding rice-specific kinesins from the cDNA library of rice prepared by NIAS and selected one, K16, for expression. The motor domain of K16 exhibited 87.4% homology with that of *Arabidopsis* plant–specific kinesin AtT·21B14.15. Although AtT·21B14.15 is an N-terminal motor domain kinesin and its full length comprises 956 amino acids, the tail domain of K16 is much shorter than that of AtT·21B14.15, resulting in a length of 547 amino acids.

Moreover, in the N-terminal region outside of the motor domain, the sequence of NRKLYNQVQDLKGS, which matches that of the consensus neck motif found among kinesins toward the minus-end of microtubules (*37*, *38*), was not observed. In addition, K16 does not have a neck linker, which has been shown to be specifically located in a plus-end directional kinesin (*39–41*). Therefore, it is strongly suggested that the primary structure of K16 is unique and that K16 may be a rice plant–specific kinesin.

As the motor domain of K16 exhibited 43.2% homology with that of mouse brain kinesin, it is expected that the enzymatic characteristics may be conserved. However, the expressed motor domain of K16 showed different ATPase activity and interaction with microtubules from in the case of mouse brain kinesin. K16 showed less microtubule-activated ATPase activity indicating lower affinity of microtubules to the binding site in the kinesin motor domain. Indeed, the K_{MT} value (5 μM) of K16 estimated from the data was approximately ten-fold higher than those of kinesin 1 (*42*, *43*). This may be explained by the observation that loop L12 in K16, which is one of the microtubule-binding sites, showed less similarity in amino acid sequence compared with in other kinesin 1. We also observed differences in loop L5 of K16 from those of kinesin 1. L5 (96–106) is one of the unique loops located in the vicinity of the ATP binding site of kinesin (*44*, *45*). We observed that point mutations in mouse brain kinesin, *e.g.*, at Leu 105 in L5, significantly affect ATPase activity (unpublished data). Moreover, the fluorescence spectrum of Trp-substituted Leu 100 in L5 was significantly altered in a nucleotide-dependent manner (unpublished data). Comparative studies on primary kinesin structures, derived from several different species, revealed that plus-end directed kinesins have longer L5 loops than minus-end directed kinesins (*44*). Therefore, loop 5 may play a key role in the direction and energy transduction of kinesin, similar to the important role in energy transduction played by loop M of myosin (*46*). Loop L5 of K16 is shorter than that of kinesin 1 suggesting that it might determine the direction of motility. Therefore, K16 might be a minus-end directed kinesin with different characteristics as to ATPase from kinesin 1.

We used a fluorescent ATP analogue, NBD-ATP, to study the conformational differences in the ATP binding site of K16 from those of other kinesins. In our previous study on mouse brain kinesin, upon the addition of kinesin to the solution of NBD-ATP, the fluorescence intensity of NBD-ATP increased rapidly by approximately 4-fold, reflecting the formation of a mouse brain kinesin•NBD-ATP complex (*14*). With regard to the *C. elegans* kinesin UNC-116 motor domain, the fluorescence intensity of

NBD-ATP also increased, but the magnitude of the enhancement was only one-tenth of that in the case of mouse brain kinesin (unpublished data). In contrast, for skeletal muscle myosin subfragment-1 (S-1), upon binding to the ATPase site, the fluorescence intensity of NBD-ATP decreased by 40% (*47*). Therefore, it was revealed that the NBD-ATP fluorophore is highly environmentally sensitive (*48*) and reflects the precise conformational differences around the ATP binding site among motor proteins (*48*). In this study, we observed 3-fold enhancement of the fluorescence intensity of NBD-ATP upon binding to the ATPase site of K16MD, which was similar in magnitude to that in the case of mouse brain kinesin. Therefore, it is thought that the conformation of the ATP binding site of K16MD is similar to that of mouse brain kinesin. In line with this observation, our recent crystallographic study of K16MD showed that the ATP binding site of K16 was extremely similar to those of kinesin 1 (unpublished data).

In conclusion, kinesin K16 has a unique primary structure and distinct enzymatic properties from other kinesins. K16 may be one of the kinesins specifically found in the rice plant. Further studies on the physiological characteristics of K16 in order to clarify their role in the plant are necessary.

We wish to thank Dr. Taiho Yamamoto (Graduate School of Science, Osaka University) for the excellent assistance in the kinetic studies with a stopped-flow apparatus.

REFERENCES

1. Bloom, G.S. and Endow, S.A. (1994) Motor proteins. 1: kinesins. *Protein Profile* **1**, 1059–1116
2. Vallee, R.B. and Shpetner, H.S. (1990) Motor proteins of cytoplasmic microtubules. *Annu. Rev. Biochem.* **59**, 909–932
3. Sawin, K.E. and Endow, S.A. (1993) Meiosis, mitosis and microtubule motors. *BioEssays* **15**, 399–407
4. Vernos, I., Raats, J., Hirano, T., Heasman, J., Karsenti, E., and Wylie, C. (1995) Xklp1, a chromosomal *Xenopus* kinesin-like protein essential for spindle organization and chromosome positioning. *Cell* **81**, 117–127
5. Vernos, I. and Karsenti, E. (1995) Chromosomes take the lead in spindle assembly. *Trends Cell Biol.* **5**, 297–301
6. Yang, J.T., Laymon, R.A., and Goldstein, L.S.B. (1989) A three-domain structure of kinesin heavy chain revealed by DNA sequence and microtubule binding analyses. *Cell* **56**, 879–889
7. Goodson, H.V., Kang, S.J., and Endow, S.A. (1994) Molecular phylogeny of the kinesin family of microtubule motor proteins. *J. Cell Sci.* **107**, 1875–1884
8. Endow, S.A., Kang, S.J., Satterwhite, L.L., Rose, M.D., Skeen, V.P., and Salmon, E.D. (1994) Yeast Kar3 is a minus-end microtubule motor protein that destabilizes microtubules preferentially at the minus ends. *EMBO J.* **13**, 2708–2713
9. Noda, Y., Sato-Yoshitake, R., Kondo, S., Nangaku, M., and Hirokawa, N. (1995) KIF2 is a new microtubule-based anterograde motor that transports membranous organelles distinct from those carried by kinesin heavy chain or KIF3A/B. *J. Cell Biol.* **129**, 157–167
10. Hirokawa, N. (1998) Kinesin and dynein superfamily proteins and the mechanism of organelle transport. *Science* **279**, 519–526
11. Nangaku, M., Sato-Yoshitake, R., Okada, Y., Noda, Y., Takemura, R., Yamazaki, H., and Hirokawa, N. (1994) KIF1B, a novel microtubule plus end-directed monomeric motor protein for transport of mitochondria. *Cell* **79**, 1209–1220
12. Hirokawa, N., Sato-Yoshitake, R., Kobayashi, N., Pfister, K.K., Bloom, G.S., and Brady, S.T. (1991) Kinesin associates with anterogradely transported membranous organelles in vivo. *J. Cell Biol.* **114**, 295–302
13. Xu, Y., Takeda, S., Nakata, T., Noda, Y., Tanaka, Y., and Hirokawa, N. (2002) Role of KIFC3 motor protein in Golgi positioning and integration. *J. Cell Biol.* **158**, 293–303
14. Shibuya, H., Kondo, K., Kimura, N., and Maruta, S. (2002) Formation and characterization of kinesin-ADP-fluorometal complexes. *J. Biochem.* **132**, 573–579
15. Nakagawa, T., Tanaka, Y., Matsuoka, E., Kondo, S., Okada, Y., Noda, Y., Kanai, Y., and Hirokawa, N. (1997) Identification and classification of 16 new kinesin superfamiliy (KIF) proteins in mouse genome. *Proc. Natl. Acad. Sci. USA* **94**, 9654–9659
16. Miki, H., Setou, M., Kaneshiro, K., and Hirokawa, N. (2001) All kinesin superfamily protein, KIF, genes in mouse and human. *Proc. Natl. Acad. Sci. USA* **98**, 7004–7011
17. Ambrose, J, C., Li, W., Marcus, A., Ma, H., and Cyr, R. (2005) A minus-end-directed kinesin with plus-end tracking protein activity is involved in spindle morphogenesis. *Mol. Biol. Cell* **16**, 1584–1592
18. Reddy, V.S. and Reddy, A.S.N. (2002) The calmodulin-binding domain from plant kinesin functions as a modular domain in conferring Ca^{2+}-calmodulin regulation to animal plus and minus-end kinesins. *J. Biol. Chem.* **277**, 48058–48065
19. Pan, R., Lee, Y.R., and Liu, B. (2004) Localization of two homologous *Arabidopsis* kinesin-related proteins in the phragmoplast. *Planta* **220**, 156–164
20. Lu, L., Lee, Y.R., Pan, R., Maloof, J.N., and Liu, B. (2005) An internal motor kinesin is associated with the Golgi apparatus and plays a role in trichome morphogenesis in *Arabidopsis*. *Mol. Biol. Cell* **16**, 811–823
21. Mitsui, H., Nakatani, K., Yamaguchi-Shinozaki, K., Shinozaki, K., Nishikawa, K., and Takahashi, H. (1994) Sequencing and characterization of the kinesin-related genes katB and katC of *Arabidopsis thaliana*. *Plant. Mol. Biol.* **25**, 865–876.
22. Reddy, A.S. and Day, I.S. (2001) Kinesin in the *Arabidopsis* genome: a comparative analysis among eularyotes. *BMC Genomics* **2**, 2
23. Cai, G., Bartalesi, A., Del Casino, C., Moscatelli, A., Tiezzi, A., and Cresti, M. (1993). The kinesin-immunoreactive homologue from *Nicotiana tabacum* pollen tube: Biochemical properties and subcellular localization. *Planta* **191**, 496–506
24. Asada, T., Kuriyama, R., and Shibaoka, H. (1997) TKRP125, a kinesin-related protein involved in the centrosome-independent organization of the cytokinetic apparatus in tobacco BY-2 cells. *J. Cell Sci.* **110**, 179–189
25. Kikuchi, S., Satoh, K., Nagata, T., Kawagashira, N., Doi, K., Kishimoto, N., Yazaki, J., Ishikawa, M., Yamada, H., Ooka, H., Hotta, I., Kojima, K., Namiki, T., Ohneda, E., Yahagi, W., Suzuki, K., Li, C. J., Ohtsuki, K., Shishiki, T., Otomo, Y., Murakami, K., Iida, Y., Sugano, S., Fujimura, T., Suzuki, Y., Tsunoda, Y., Kurosaki, T., Kodama, T., Masuda, H., Kobayashi, M., Xie, Q., Lu, M., Narikawa, R., Sugiyama, A., Mizuno, K., Yokomizo, S., Niikura, J., Ikeda, R., Ishibiki, J., Kawamata, M., Yoshimura, A., Miura, J., Kusumegi, T., Oka, M., Ryu, R., Ueda, M., Matsubara, K., Kawai, J., Carninci, P., Adachi, J., Aizawa, K., Arakawa, T., Fukuda, S., Hara, A., Hashizume, W., Hayatsu, N., Imotani, K., Ishii, Y., Itoh, M., Kagawa, I., Kondo, S., Konno, H., Miyazaki, A., Osato, N., Ota, Y., Saito, R., Sasaki, D., Sato, K., Shibata, K., Shinagawa, A., Shiraki, T., Yoshino, M., Hayashizaki, Y., Yasunishi, A.; Rice Full-Length cDNA Consortium; National Institute of Agrobiological Sciences Rice Full-Length cDNA Project Team; Foundation of Advancement of International Science Genome

Sequencing & Analysis Group; RIKEN (2003) Collection, mapping, and annotation of over 28,000 cDNA clones from *japonica* rice. *Science* **301**, 376–379
26. Sasaki, T., Matsumoto, T., Yamamoto, K., Sakata, K., Baba, T., Katayose, Y., Wu, J., Niimura, Y., Cheng, Z., Nagamura, Y., Antonio, B. A., Kanamori, H., Hosokawa, S., Masukawa, M., Arikawa, K., Chiden, Y., Hayashi, M., Okamoto, M., Ando, T., Aoki, H., Arita, K., Hamada, M., Harada, C., Hijishita, S., Honda, M., Ichikawa, Y., Idonuma, A., Iijima, M., Ikeda, M., Ikeno, M., Ito, S., Ito, T., Ito, Y., Ito, Y., Iwabuchi, A., Kamiya, K., Karasawa, W., Katagiri, S., Kikuta, A., Kobayashi, N., Kono, I., Machita, K., Maehara, T., Mizuno, H., Mizubayashi, T., Mukai, Y., Nagasaki, H., Nakashima, M., Nakama, Y., Nakamichi, Y., Nakamura, M., Namiki, N., Negishi, M., Ohta, I., Ono, N., Saji, S., Sakai, K., Shibata, M., Shimokawa, T., Shomura, A., Song, J., Takazaki, Y., Terasawa, K., Tsuji, K., Waki, K., Yamagata, H., Yamane, H., Yoshiki, S., Yoshihara, R., Yukawa, K., Zhong, H., Iwama, H., Endo, T., Ito, H., Hahn, J. H., Kim, H. I., Eun, M. Y., Yano, M., Jiang, J., and Gojobori, T. (2002) The genome sequence and structure of rice chromosome 1. *Nature* **420**, 312–316
27. Laemmli, U.K. (1970) Cleavage of structural proteins during the assembly of the head of bacteriophage T4. *Nature* **227**, 680–685
28. Hackney, D.D. (1988) Kinesin ATPase: Rate-limiting ADP release. *Proc. Natl. Acad. Sci USA* **85**, 6314–6318
29. Youngburg, G.E. and Youngburg, M.V. (1930) A system of blood phosphorus analysis. *J. Lab. Clin. Med.* **16**, 158–166
30. Lockhart, A., Crevel I.M., and Cross, R.A. (1995) Kinesin and ncd bind through a single head to microtubules and compete for a shared MT binding site. *J. Mol. Biol.* **249**, 763–771
31. Maruta, S., Mizukura, Y., and Chaen, S. (2002) Interaction of a new fluorescent ATP analogue with skeletal muscle myosin subfragment-1. *J. Biochem*. **131**, 905–911
32. Kull, F.J., Sablin, E.P., Lau, R., Fletterick, R.J., and Vale, R.D. (1996) Crystal structure of the kinesin motor domain reveals a structural similarity to myosin. *Nature* **380**, 550–555
33. Ma, Y.Z. and Taylor, E.W. (1997) Kinetic mechanism of a monomeric kinesin construct. *J. Biol. Chem.* **272**, 717–723.
34. Bowser, J. and Reddy, A.S.N. (1997) Localization of a kinesin-like calmodulin-binding protein in dividing cells of *Arabidopsis* and tobacco. *Plant J.* **12**, 1429–1437
35. Lee, Y.R.J., Giang, H.M., and Liu, B. (2001) A novel plant kinesin-related protein specifically associates with the phragmoplast organelles. *Plant Cell* **13**, 2427–2439
36. Reddy, V.S., Day, I.S., Thomas, T., and Reddy, A.S.N. (2004) KIC, a novel Ca^{2+} binding protein with one EF-hand motif, interact with a microtubule motor protein and regulates trichome morphogenesis. *Plant Cell* **16**, 185–200
37. Endow, S.A. (1999) Determinants of molecular motor directionality. *Nat. Cell. Biol.* **1**, E163–E167
38. Preuss, M.L., Kovar, D.R., Lee, Y.R., Staiger, C.J., Delmer, D.P., and Liu, B. (2004) A plant-specific kinesin binds to actin microfilaments and interacts with cortical microtubules in cotton fibers. *Plant Physiol.* **136**, 3945–3955
39. Case, R.B., Pierce, D.W., Hom-Booher, N., Hart, C.L., and Vale, R.D. (1997) The directional preference of kinesin motors is specified by an element outside of the motor catalytic domain. *Cell* **90**, 959–966
40. Henningsen, U. and Schliwa, M. (1997) Reversal in the direction of movement of a molecular motor. *Nature* **389**, 93–96
41. Endow, S.A. and Waligora, K.W. (1998) Determinants of kinesin motor polarity. *Science* **281**, 1200–1202
42. Klumpp, L.M., Brendza, K.M., Rosenberg, J.M., Hoenger, A., and Gilbert, S.P. (2003) Motor domain mutation traps kinesin as a microtubule rigor complex. *Biochemistry* **42**, 2595–606
43. Ma, Y.Z. and Taylor, E.W. (1995) Mechanism of microtubule kinesin ATPase. *Biochemistry* **34**, 13242–13251
44. Song, Y.H., Marx, A., Muller, J., Woehlke, G., Schliwa, M., Krebs, A., Hoenger, A., and Mandelkow, E. (2001) Structure of a fast kinesin: implications for ATPase mechanism and interactions with microtubules. *EMBO J.* **20**, 6213–6225
45. Endow, S.A. and Komma, D.J. (1997) Spindle dynamics during meiosis in *Drosophila* Oocytes. *J. Cell. Biol.* **137**, 1321–1336
46. Maruta, S. and Homma, K. (2000) Conformational changes in the unique loops bordering the ATP binding clef of skeletal muscle myosin mediate energy transduction. *J. Biochem.* **128**, 695–704
47. Maruta, S., Mizukura, S., and Chaen, S. (2002) Interaction of a new fluorescent ATP analogue skeletal muscle myosin subfragment-1. *J. Biochem.* **132**, 905–911
48. Chattopadhyay, A. (1990) Chemistry and biology of N-(7-nitro-benz-2-oxa-1,3-diazol-4-yl)-labeled lipids: fluorescent probe of biological and model membranes. *Chem. Phys. Lipids* **53**, 1–15